

DISSERTATION

BARIUM TAGGING IN SOLID XENON FOR THE NEXO NEUTRINOLESS DOUBLE BETA
DECAY EXPERIMENT

Submitted by

Timothy Walton

Department of Physics

In partial fulfillment of the requirements

For the Degree of Doctor of Philosophy

Colorado State University

Fort Collins, Colorado

Fall 2015

Doctoral Committee:

Advisor: William M. Fairbank, Jr.

Robert Wilson
Bruce Berger
Alan Van Orden

Copyright by Timothy Walton 2015

All Rights Reserved

ABSTRACT

abztrakt

ACKNOWLEDGEMENTS

Bill, Chris for all the help in the lab and building things, Shon and Brian for creating the system and training me (Shon) and for the preliminary results, Adam, Cesar, Kendy.

If you want the Leif thing, uncomment it in csuthesis.cls. It says something like "this dissertation is typeset in ... designed by Leif Anderson.

Jamie and LEW, and other fam.

TABLE OF CONTENTS

Abstract	ii
Acknowledgements	iii
Chapter 1. Introduction	1
1.1. Neutrinos	2
1.2. Enriched Xenon Observatory	7
Chapter 2. Theory	17
2.1. Barium Spectroscopy	17
2.2. Matrix Isolation Spectroscopy	17
Chapter 3. Apparatus	18
3.1. Ion Beam	18
3.2. Ba Getter Source	20
3.3. Solid Xenon Matrix Deposition	21
Chapter 4. Results	22
Chapter 5. Conclusions	23
Appendix A. Supplementary Material	24
A.1. Some Sample Material	24
Appendix B. Another Supplement	25

CHAPTER 1

INTRODUCTION

Neutrinos have provided illumination as well as great challenge to physics since their discovery. They first entered our consciousness through W. Pauli, who proposed in 1930 the existence of a neutral, unobserved particle to explain the apparent violation of energy conservation in beta decay. He admitted that neutrinos (then deemed “neutrons” – what we now know as neutrons had not been discovered yet either) should be difficult to observe experimentally, but also that it seemed unlikely that they would never have been noticed before [ref: Pauli letter, or a following paper?]. As it turns out, they are much more difficult to observe than he predicted; they aren’t likely to be noticed without extreme experimental techniques.

A theory formulated in 1933 by E. Fermi for beta decay, including the neutrino, would be the beginnings of weak theory, and the development of the very successful Standard Model of particle physics. But neutrinos continued to challenge theory with the discovery of non-zero neutrino mass, and they remain at the forefront of our exploration of the universe.

The possibility that neutrinos are Majorana particles makes the search for neutrinoless double beta decay very important for the further development of particle theory. Majorana formulation can describe the origin of neutrino mass, and possibly explain why the mass is very small via the Seesaw Mechanism [ref]. Observation of neutrinoless double beta decay would simultaneously demonstrate that neutrinos are Majorana particles, as well as give a measurement of the absolute mass itself [ref? this is said later too].

To motivate barium tagging, this chapter outlines the current theory for neutrinos, and then describes the neutrinoless double beta decay experiments EXO-200 and nEXO.

1.1. NEUTRINOS

Neutrinos are chargeless leptons which only interact via the weak force (and gravity). There are three known “flavors” of neutrinos, each corresponding to one of the three known leptons: ν_e , ν_μ , and ν_τ . These are the eigenstates in the basis of the weak force, so they are the states in which a neutrino will interact via the weak force.

1.1.1. NEUTRINO OSCILLATION AND MASS. The postulate that neutrinos have an energy basis which is different from the flavor basis predicts the phenomenon of oscillation – that the time evolution of an initially pure flavor state (as a neutrino will be produced) will result in a time-dependent probability of measuring the other two flavors as well.

The very small mass of a neutrino (assumed zero in the SM), specifically relative to its momentum, lets one write its Hamiltonian in terms of mass squared differences $\Delta m_{ij}^2 = m_i^2 - m_j^2$, where $i, j = 1, 2, 3$, referring to what we then call mass states. The mass basis is really the energy basis with the small mass approximation, along with dropping some constant terms in the Hamiltonian (which do not affect time evolution). Writing the time evolution in terms of mass squared differences means that neutrino oscillation experiments can produce measurements of these differences. In fact, the discovery of neutrino oscillation was the first (and only, so far) demonstration that neutrinos have a non-zero mass. Without neutrino mass (particularly without differences between the masses of the mass states), neutrinos would not oscillate.

Neutrino oscillation experiments also provide measurements on the amount of mixing between the flavor basis and the mass basis. We define the mixing between them by a rotation in terms of three mixing angles, θ_{12} , θ_{23} , and θ_{13} . Transformation between the

flavor and mass bases is done with the following unitary matrix, called the Pontecorvo–Maki-Nakagawa-Sakata (PMNS) matrix:

$$\begin{aligned}
 (1) \quad U &= \begin{pmatrix} 1 & 0 & 0 \\ 0 & c_{23} & s_{23} \\ 0 & -s_{23} & c_{23} \end{pmatrix} \begin{pmatrix} c_{13} & 0 & s_{13}e^{-i\delta} \\ 0 & 1 & 0 \\ -s_{13}e^{i\delta} & 0 & c_{13} \end{pmatrix} \begin{pmatrix} c_{12} & s_{12} & 0 \\ -s_{12} & c_{12} & 0 \\ 0 & 0 & 1 \end{pmatrix} \begin{pmatrix} 1 & 0 & 0 \\ 0 & e^{i\alpha_1/2} & 0 \\ 0 & 0 & e^{i\alpha_2/2} \end{pmatrix} \\
 &= \begin{pmatrix} c_{12}c_{13} & s_{12}c_{13} & s_{13}e^{-i\delta} \\ -s_{12}c_{23} - c_{12}s_{23}s_{13}e^{i\delta} & c_{12}c_{23} - s_{12}s_{23}s_{13}e^{i\delta} & s_{23}c_{13} \\ s_{12}s_{23} - c_{12}c_{23}s_{13}e^{i\delta} & -c_{12}s_{23} - s_{12}c_{23}s_{13}e^{i\delta} & c_{23}c_{13} \end{pmatrix} \begin{pmatrix} 1 & 0 & 0 \\ 0 & e^{i\alpha_1/2} & 0 \\ 0 & 0 & e^{i\alpha_2/2} \end{pmatrix}
 \end{aligned}$$

where $c_{ij} = \cos \theta_{ij}$ and $s_{ij} = \sin \theta_{ij}$. δ is a phase factor related to lepton CP violation, and α_i are Majorana phases.

Studying oscillations of neutrinos from different kinds of sources, with different energies and path lengths, can isolate sensitivities to the different parameters. For example, the study of solar neutrinos (neutrinos emanating from nuclear fusion reactions in the core of the sun) provides sensitivity to θ_{12} and Δm_{12}^2 (*right? θ_{12} may not be specifically solar...*). Beamline neutrino detectors can be designed for maximum sensitivity to parameters. The parameters so far measured are as follows in Table 1.1:

TABLE 1.1. up to date values with references, and denote “solar”, “atmos.”, etc.

Parameter	Measurement
Δm_{12}^2	
$ \Delta m_{31}^2 $	
$\sin^2 \theta_{12}$	
$\sin^2 \theta_{23}$	
$\sin^2 \theta_{13}$	

Note that only the absolute value of Δm_{31}^2 is known. As a consequence, there are two possibilities for the hierarchy of the three neutrino masses. These are called the Normal and Inverted Hierarchies, as shown in Fig. 1.1.

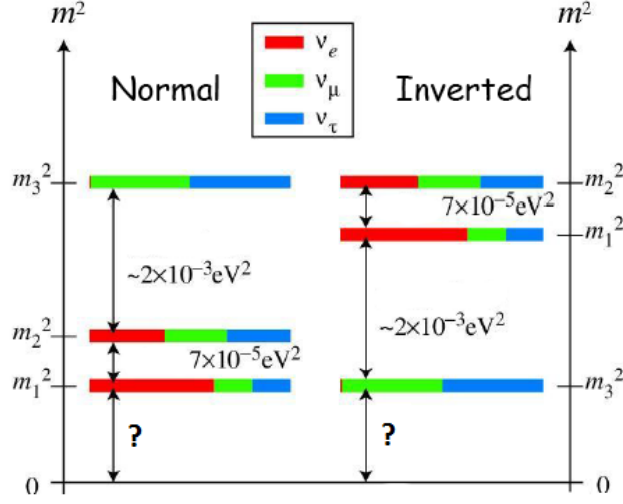


FIGURE 1.1. The two possible hierarchies of neutrino masses. The colors depict the mixing between the mass and flavor bases. [ref]

The correct mass hierarchy remains unknown, but next-generation neutrino experiments, possibly including nEXO, will be able to discern this.

Neutrino oscillation demonstrates that neutrinos have non-zero mass, and though oscillation experiments can measure the mass squared differences, we still do not have a measurement of the absolute masses of the three neutrinos.

Neutrinoless double beta decay experiments like EXO-200 search for specifically the Majorana neutrino mass (i.e., neutrino mass if neutrinos are indeed Majorana particles). Cosmology can put limits on the sum of the three neutrino masses, the current limit of which is [??] [ref planck or something else]. The KATRIN experiment aims to measure the neutrino mass by accurately observing the spectrum of tritium beta decay near the Q-value [ref KATRIN].

Neutrino oscillation and non-zero neutrino mass are physics beyond the Standard Model (SM) of particle physics, and though much has been discovered through oscillation experiments, there is much yet to learn about neutrinos. Since they are chargeless, they may be Majorana particles, and their small mass could be explained by the See-saw Mechanism [ref]. Majorana particles are their own anti-particle, and this, along with the discovery that neutrinos have mass, allows for a unique test of the Majorana (vs. Dirac) nature of neutrinos: neutrinoless double beta decay.

1.1.2. NEUTRINOLESS DOUBLE BETA DECAY. Double beta decay is the simultaneous emission of two electrons from a nucleus. Two-neutrino double beta decay, shown in Fig. 1.2(left), is allowed by the Standard Model and has been observed in several isotopes which are listed in Table 1.2. Similar to beta decay, a neutrino accompanies each electron in this decay, broadening the spectrum of the summed electron energy. This is a second-order process, making it a rare decay, and requiring low backgrounds to measure.



FIGURE 1.2. Two-neutrino (left) and Neutrinoless (right) double beta decay.

Neutrinoless double beta decay, shown in Fig. 1.2(right), is a postulated mode of double beta decay. In this case, the neutrino is exchanged as a virtual particle (which would require that it is a Majorana particle), and there are no neutrinos in the final products. If discovered, not only would neutrinos be determined Majorana particles, but their absolute mass could also be measured in the form of an effective electron neutrino mass, since the rate of neutrinoless double beta decay will depend on the absolute neutrino mass as shown in Eqn. 2:

$$(2) \quad T_{1/2}^{0\nu} = (G^{0\nu}(Q, Z)|M^{0\nu}|^2 \langle m_\nu \rangle^2)^{-1}$$

where $T_{1/2}^{0\nu}$ is the $0\nu\beta\beta$ half-life, $G^{0\nu}$ is a known phase space factor, and $M^{0\nu}$ is a model-dependent nuclear matrix element. The effective electron neutrino mass $\langle m_\nu \rangle$ is the expectation value of the mass for a pure electron neutrino:

$$(3) \quad \langle m_\nu \rangle = \sum_i U_{ei}^2 m_i.$$

The sum of the energies of the emitted electrons in double beta decay will serve as the distinction between the two-neutrino and zero-neutrino modes, shown in Fig. 1.3. In the two-neutrino mode, the total decay energy is shared probabilistically between the electrons and the neutrinos (the nucleus recoil energy is negligible), resulting in a broad distribution in the summed electron energy. (Recall the similarly broad electron energy in single beta decay, which ultimately led to discovery of the neutrino involved.) But in the zero-neutrino mode, all of the decay energy is carried away by the two electrons, resulting in only a single allowed

value for the summed electron energy – a peak in the summed electron energy spectrum at the Q-value.

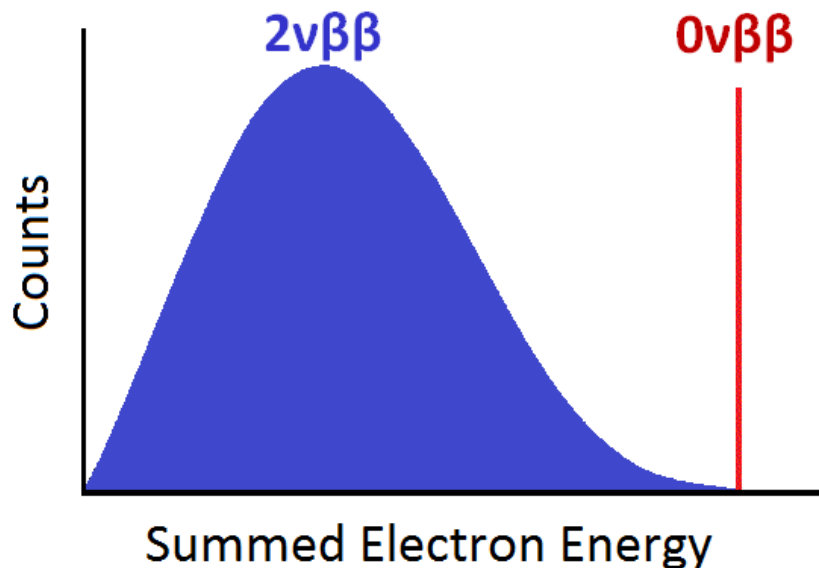


FIGURE 1.3. Conceptual two-neutrino (blue) and zero-neutrino (red) double beta decay spectra.

TABLE 1.2. $2\nu\beta\beta$ half-lives measured for various isotopes.

Isotope	Experiment	$T_{1/2}^{2\nu}$
Xe ₁₃₆	EXO-200	2.
...

The rarity of double beta decay (see the very long half lives in Table 1.2) requires very low backgrounds, especially around the Q-value for the $0\nu\beta\beta$ search. The next sections describe EXO-200 and it’s next-generation successor, nEXO.

1.2. ENRICHED XENON OBSERVATORY

The Enriched Xenon Observatory (EXO) is a set of two experiments, each a LXe time projection chamber (TPC) designed to study the double beta decay of the isotope ^{136}Xe , and ultimately to search for the zero-neutrino mode. There are several advantages to a LXe detector. Xe is extremely transparent, and scintillates at [around?] [xxx] nm, which is

[efficiently collected by [type that the APDs are]] [reference]; so the Xe acts as a detection medium in addition to being the source of the double beta decay [reference? I didn't make up that kind of sentence]. Xe can be continuously purified to maintain large electron lifetimes in the LXe. Also, the ratio between observed scintillation light and remaining ionized electrons (drifted from the decay site by the TPC's electric field) exhibits a well-known microscopic anti-correlation [ref.], the understanding of which improves the energy resolution of the detector. Finally, a LXe TPC approach offers the opportunity, [fairly] unique in double beta decay, to reach in and identify, or “tag”, the daughter Ba^{++} at the site of the double beta decay event, which would provide a background-free identification of neutrinoless double beta decay. Barium tagging is the focus of our group at CSU and is the subject of this thesis.

The following sections describe the EXO-200 experiment, as well as nEXO, the next-generation tonne-scale LXe TPC which is now in the design stages. EXO-200 does not have barium tagging implemented, but it is hoped that nEXO will.

1.2.1. EXO-200. EXO-200 has been operational since April of 20[xx](?). It is a LXe TPC designed to probe Majorana neutrino masses down to around 100 meV [EXO instrum. paper part I], and is located about half a mile underground in the Waste Isolation Pilot Plant (WIPP) near Carlsbad, NM. This mine is in a salt basin, which contains lower levels of Uranium and Thorium than a typical mine in rock, making it more ideal for a low-background experiment. WIPP's main purpose is to permanently store transuranic nuclear waste, which is stored at the other end of the mine and is not an issue for EXO-200.

A schematic of the TPC in the class 100 cleanroom is shown in Fig. 1.4. Several layers of lead wall surround the copper cryostat, which is filled with hydro-fluoro-ethylwhatever

(HFE), a cryogenic fluid which keeps the TPC cooled to LXe temperatures, as well as aids in shielding. The copper material of the cryostat and TPC is [purified or something?], and is kept as thin as possible to minimize backgrounds.

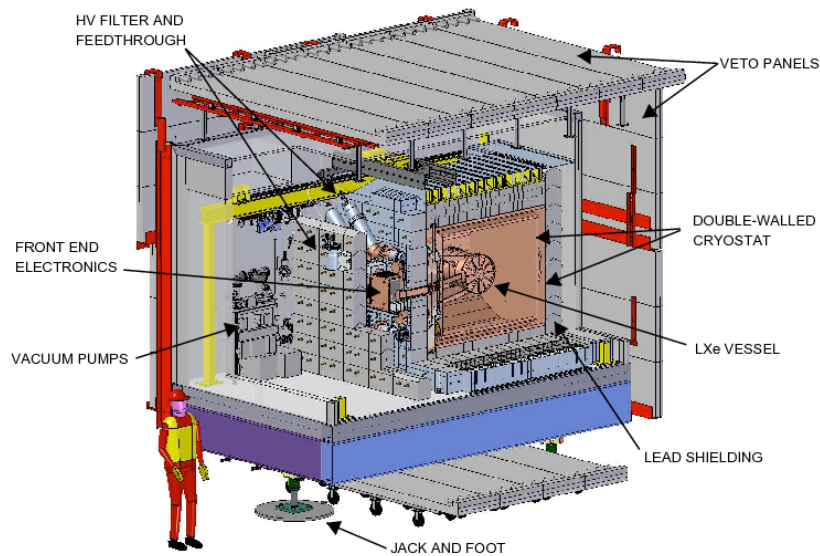


FIGURE 1.4. Drawing of cleanroom laboratory in the WIPP drift. **Find better-rez pic.**

Fig. 1.5 shows the EXO-200 detector. It is actually two face-to-face TPCs which share a cathode. The detection planes are a combination of ionized charge induction/collection wires and avalanche photodiodes which detect scintillation light.

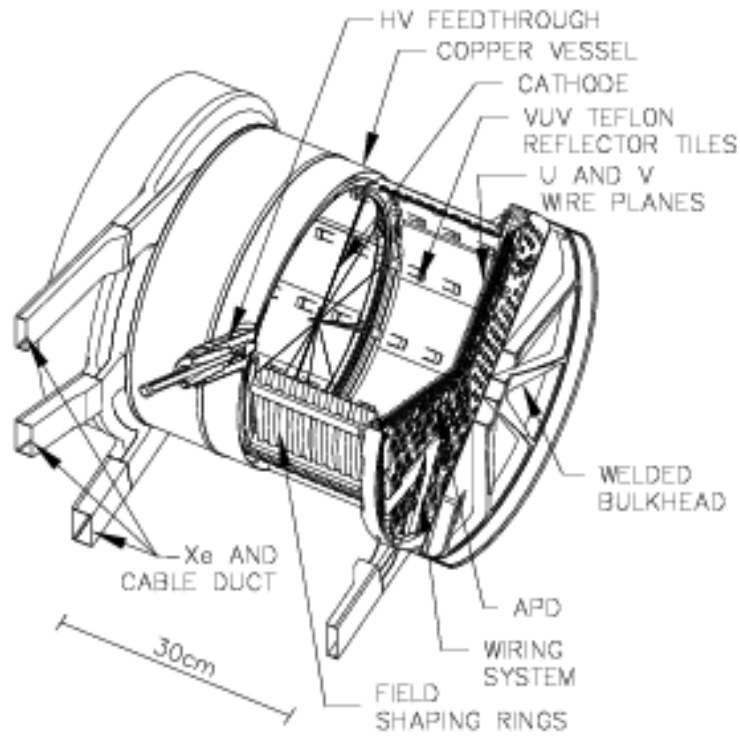


FIGURE 1.5. EXO-200 TPC diagram. [ref 0ν paper or whatev] **Better rez of this too?**

A photograph of the detection plane is shown in Fig. 1.6, and a schematic of event detection is shown in Fig. 1.7. When a double beta decay event occurs in the LXe, the energetic electrons ionize many surrounding Xe atoms. Some electrons very quickly recombine, emitting scintillation light which is collected by the APDs. This is part of the energy collection, and also provides a time stamp for the event.

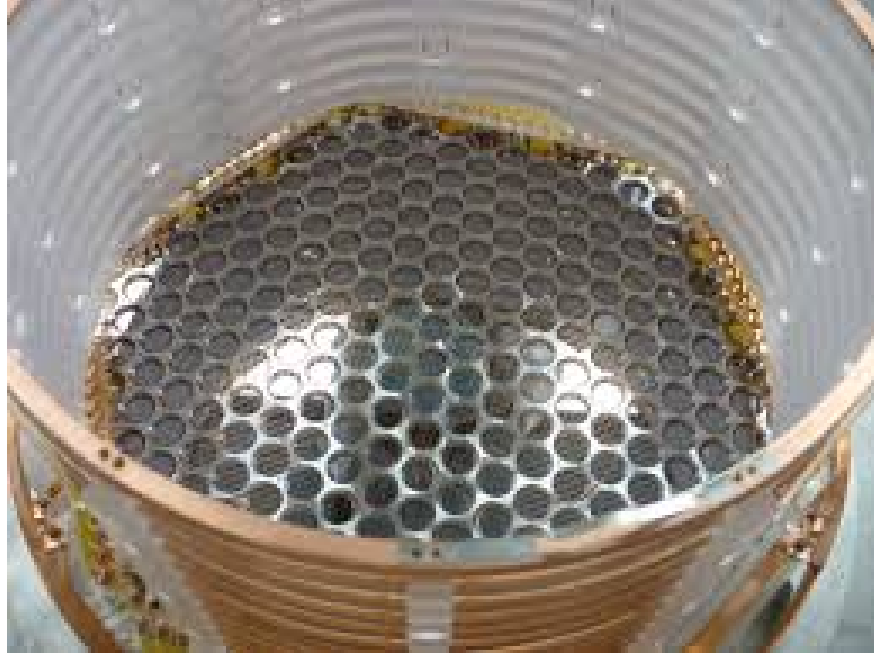


FIGURE 1.6. View of the detection plane in one of the two EXO-200 TPCs.
[ref 0ν paper or whatev] **I know you have a better rez of this.**

The cathode is set to 8 kV, providing an electric field of [xxx] V/cm across the 20 cm drift length of each TPC. Ionized electrons drift from the decay site, first passing the v-wires, which receive an induction signal, and are then collected by the u-wires, which are set at a 60° angle from the v-wires. The charge collection provides the remainder of the energy collection of the initial decay.



FIGURE 1.7. EXO-200 event detection.

Together, the u- and v-wires give an x/y position measurement for the event. The time between the initial scintillation detection and the charge collection give a z position, and a 3D position can be reconstructed for the event.

Having a reconstructed 3D event position is important in several ways. Firstly, position-based corrections on scintillation and charge collection can be applied. For charge, electronegative impurities in the LXe will absorb the drifting charge, requiring a drift-length (z-position) correction. High purity levels, measured in terms of electron lifetime, of [??] are maintained in EXO-200, but a small correction of [??] must still be applied [ref]. For scintillation, a full 3D correction is applied (called the Light Map), as some regions have more efficient light collection by the APDs [ref, maybe for whole paragraph].

A 3D position also allows a fiducial volume to be defined. The materials of the Teflon walls and cathode/detection planes contain more radioactive background-producing elements. Radioactive daughters from impurities like radon in the LXe bulk also tend to collect of the cathode [ref], so a stand-off distance of [??] is used as the fiducial cut.

Finally, 3D reconstruction allows the distinction between single-site (SS) and multi-site (MS) events. A(n?) MS event is one where two spatially separated events occur in the same [??]- μs time window. These are mostly caused by gamma rays interacting in the LXe, which can Compton-scatter several times. Rejecting MS events strongly separates gamma events from double beta decay events.

Of course, barium tagging will also require a 3D reconstructed position in nEXO.

Calibration of EXO-200 is done using various radioactive sources which can be moved to several positions around the outside of the TPC. Several different sources span the energy range of interest, but the main source is Th_{228} , which produces gamma rays at [??] MeV, near the Q-value of Xe_{136} double beta decay where the $0\nu\beta\beta$ peak will be. Source calibration data also provides a comparison between data and Monet-Carlo simulation, and provides the data for purity measurement and Light Map determination. Data and Monte-Carlo for Th_{228} are shown in Fig. [ref fig source agreement].

The relationship between scintillation and ionization for a given event in LXe exhibits a well-known anti-correlation. Applying this to the combination of those signals improves the energy resolution, shown in Fig. [ref fig anticorrelation]. This correction defines a combined energy axis, called the rotated energy. Energy resolution is important in a $0\nu\beta\beta$ search, as it distinguished those events from $2\nu\beta\beta$ events in the tail of their spectrum. Resolution of [??] is achieved in [ref 0ν paper].

The final data set is fit using a combination of probability distribution functions (PDFs) for $0\nu\beta\beta$, $2\nu\beta\beta$, and all possible backgrounds. Fig. 1.8 shows the fits to the final energy spectrum data for (a) SS events, and (b) MS events. The green bands beneath each plot show the residuals vs. energy. The $2\nu\beta\beta$ spectrum, in gray, dominates the backgrounds in the SS spectrum. The red dotted lines in the SS spectrum outline the 2σ region of interest around the Q-value, where the $0\nu\beta\beta$ peak will lie. The insets are a zoom into this region. The fit value for $0\nu\beta\beta$ in this dataset is non-zero, but it is not statistically significant enough to claim discovery [ref nature].

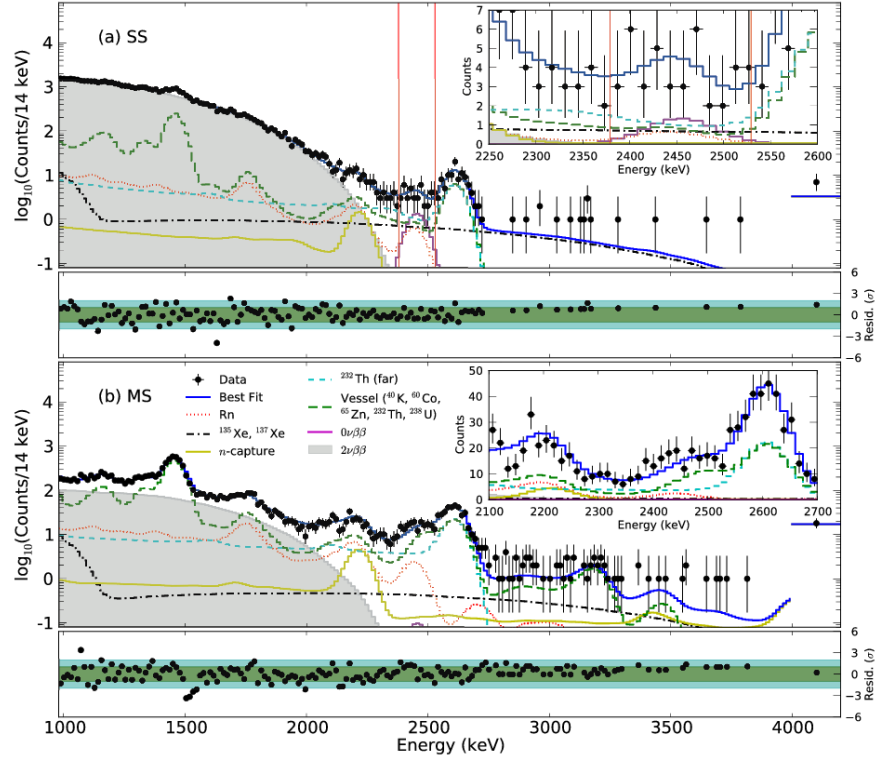


FIGURE 1.8. EXO-200 energy spectrum.

[ref nature] reports the most accurate measurement of the $2\nu\beta\beta$ of Xe_{136} to date, at [???], and reports a limit on the half-life of $0\nu\beta\beta$ of Xe_{136} of [???] at the 95 % confidence level,

which translates to an upper limit on the Majorana neutrino mass between [??] and [??], depending on the method of calculation for [which param?].

1.2.2. nEXO. The next-generation successor to EXO-200 is nEXO, a tonne-scale LXe TPC which will probe Majorana neutrino masses down to the [??] scale [ref]. The sensitivity projections for nEXO are shown in Fig. 1.9, along with those of EXO-200. nEXO will reach phase space where the two possible mass hierarchies begin to split; if nEXO successfully observes $0\nu\beta\beta$ in these regions, it may be able to also determine the mass hierarchy. Barium tagging will push the sensitivity further into the region allowed only by the normal hierarchy [ref for this?].

A schematic of the experimental setup is shown in Fig. [fig cryopit] in one of the possible locations for nEXO, the SNOLab cryopit. Similar to EXO-200, the copper-housed TPC will be submerged in HFE fluid, inside a copper cryostat. The cryostat is insulated and submerged in a large volume of water shielding. Photo-multiplier tubes in the water tank can provide muon veto by observing Cherenkov radiation.

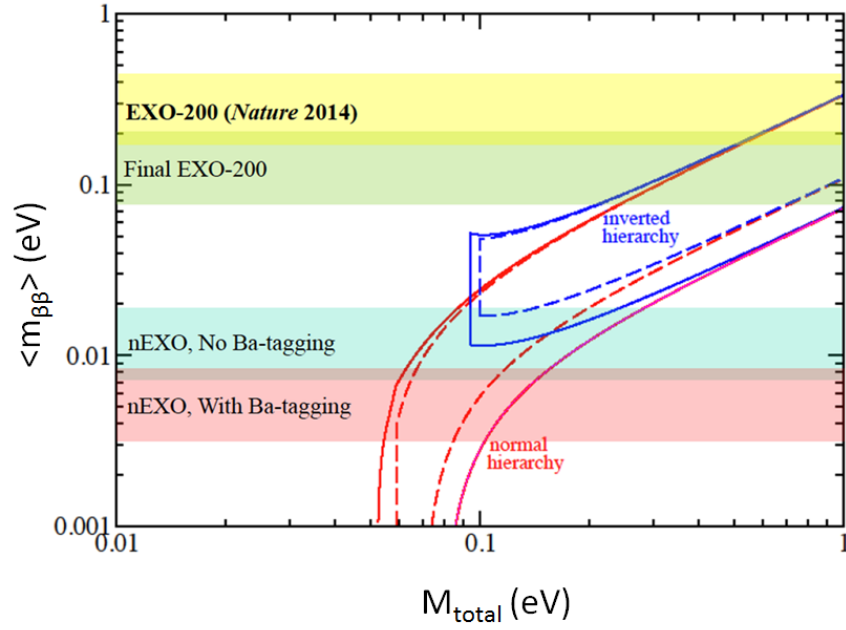


FIGURE 1.9. nEXO projected sensitivity to the Majorana neutrino mass vs. the sum of the three masses M_{total} .

nEXO will be a single TPC with charge and light readouts at opposing ends of the TPC.

1.2.3. BARIUM TAGGING.

CHAPTER 2

THEORY

Theory relevant to the spectroscopy of Ba in SXe is discussed.

2.1. BARIUM SPECTROSCOPY

Do we want this here? It flows more to have this theory after the proposition of the tagging technique, but maybe that's more appropriate for a talk.

2.2. MATRIX ISOLATION SPECTROSCOPY

(same thing)

CHAPTER 3

APPARATUS

Should data results of diagnostic stuff, like Ba^+ velocity (from pulses), be in this chapter?

This chapter describes the apparatus at Colorado State University, which we have used for all described studies of Ba fluorescence in SXe after deposition in vacuum. Our main Ba source, the Ba^+ ion source/beam, is first described, as well as the measurements (using Faraday cups) used for determining the number of ions we deposit. A purely Ba neutral source is described. The co-deposit of Ba/ Ba^+ with Xe gas onto a cold sapphire window, subsequent laser excitation, and finally the collection optics for the fluorescence, are described.

3.1. ION BEAM

3.1.1. BARIUM ION SOURCE/ACCELERATION. Barium ions are produced in a Colutron [type?] ion gun system [reference], as depicted in Fig. x. A solid barium charge is placed into the hollowed end of a stainless steel rod, which is then inserted into the discharge chamber, near the hot filament. The heated barium vaporizes, allowed to escape the hollowed rod around a loosely threaded set screw at the end of the rod. The discharge chamber then fills with barium vapor. A voltage is applied to the anode plate, which then creates a discharge, through the barium vapor, between the anode and the filament. The resulting plasma, containing barium ions, then escapes through the small hole in the anode plate, where it enters the acceleration potential.

The acceleration potential is 2 kV, between the ion source anode and an aperture, which constitutes the first element of the "acceleration lens" (Fig. 3.1). The acceleration lens is an

Einzel lens, the voltages for which are chosen to approximately collimate the ion beam for passage through the $E \times B$ velocity filter.



FIGURE 3.1. figyer

3.1.2. VELOCITY FILTER, LENSING. The $E \times B$ velocity filter selects Ba^+ by providing perpendicular electric and magnetic fields, which produce opposing forces on charged particles moving straight through the filter. Those fields are chosen such that those forces are equal for Ba^+ , according to Eqn. 4:

$$(4) \quad \sigma = 1.$$

Other ions will be deflected, while Ba^+ will continue along the beam path.

The full ion beam is shown in Fig. xxx. The Decelerator lens can be used to reduce the beam energy, but is not needed for 2 keV beams, which are used in this work. Einzel Lens 3

focuses the beam onto the main Faraday cup, which is used during experiments to measure ion current. The final set of deflection plates, H2 and V2, are also used during experiments to steer the beam for deposits.

3.1.3. ION BEAM PULSING. To deposit small numbers of ions in a controlled manner, a set of pulsing plates can be used (Fig. xxxx). When running in this mode, the pulsing plates are first placed at 200 V and -200 V to deflect the beam, and are pulsed to 0 V for $1\ \mu\text{s}$ for each pulse.

The pulses can be detected by the Induction Plates. Since they use induction, they can be used to observe the pulses during an ion deposition (unlike using the Faraday cup to measure ion current during a DC deposit). An example of an oscilloscope readout of the pulsing plate signal and subsequent induction plate signal, is shown in Fig. 5x.

3.2. BA GETTER SOURCE

Ba "getters" are typically used in vacuum systems to improve vacuum by emitting Ba atoms, which grab gas molecules and hold them to the chamber walls. We employ getters as a neutral Ba source in our system.

...

It is very helpful to have a completely different type of Ba source, to rule out any source-related quirks, e.g. source-produced impurities.

3.3. SOLID XENON MATRIX DEPOSITION

The final destination of the barium ions is in the solid xenon matrix, which is deposited onto a cold sapphire window. Sapphire has good thermal conductivity, good optical transparency in the visible, and does not fluoresce in the wavelength region where barium fluoresces.

Xenon freezes around 73 K (?) at our pressures ($0.5 - 1 \times 10^{-7}$ Torr), so the window is cooled to temperatures below that. The window is held to a cold finger (Fig. 6x, picture of), cooled by a -brand- cryostat.

3.3.1. DEPOSITION PROCEDURE. Before barium ions are let through, xenon gas is allowed to flow, controlled by a leak valve, onto the cold sapphire window, where it freezes and begins growing the solid matrix. The Faraday cup is then retracted, to clear the path for barium ions. The cup serves as a shutter for DC deposition, or if pulsing is being used, they are performed at this time. Barium ions land in the solid xenon as the matrix continues to grow. The cup is then replaced, and the xenon leak stopped.

CHAPTER 4

RESULTS

CHAPTER 5

CONCLUSIONS

Ba⁺

APPENDIX A

SUPPLEMENTARY MATERIAL

make these also into separate files plz

A.1. SOME SAMPLE MATERIAL

Did the name for the written material come before the name of the organ? Here [?] is a citation in an appendix.

APPENDIX B

ANOTHER SUPPLEMENT